Organic Electronics 12 (2011) 886–890

Contents lists available at ScienceDirect

Organic Electronics

journal homepage: www.elsevier.com/locate/orgel

Enhanced omnidirectional photon coupling via quasi-periodic patterning of indium-tin-oxide for organic thin-film solar cells

Ping-Chen Tseng [a], Min-Hsiang Hsu [a], Min-An Tsai [b], Chih-Wei Chu [c], Hao-Chung Kuo [a], Peichen Yu [a,*]

[a] Department of Photonics and Institute of Electro-Optical Engineering, National Chiao Tung University, Hsinchu 30010, Taiwan, ROC
[b] Department of Electro-Physics, National Chiao Tung University, Hsinchu 30010, Taiwan, ROC
[c] Research Center for Applied Sciences, Academia Sinica, Taipei 11529, Taiwan, ROC

ARTICLE INFO

Article history:
Received 18 November 2010
Received in revised form 3 February 2011
Accepted 6 March 2011
Available online 21 March 2011

Keywords:
Optical coupling
Omnidirectional
Thin-film solar cell

ABSTRACT

Enhanced optical coupling via an indium tin oxide quasi-periodic structure (ITO-QPS) as the frontal electrode for organic thin film solar cells was demonstrated. The QPS was fabricated via scalable polystyrene colloidal lithography, which effectively coupled the incident light to the photo-active layer through antireflection and light-trapping mechanisms. The cell efficiency was boosted from 2.91% to 3.26%, corresponding to a 12% enhancement after ITO patterning. Moreover, the angle-resolved absorption spectroscopy also confirmed excellent light coupling at large angles of incidence to 45°, particularly in the wavelength range between 540 and 670 nm. The ITO-QPS guarantees broadband and omnidirectional light harvesting and is widely applicable to a variety of thin film solar cells.

1. Introduction

Thin-film solar cells offer the benefits of reduced material and fabrication costs and the convenience of large-area fabrication in the industrial production [1]. However, for thin-film structures the short optical absorption length and insufficient optical coupling into the thin active layer are the major challenges. The design for the high photon absorption usually requires relatively thick active layers, which results in poor carrier collection efficiencies [2–5]. Geometries that sufficiently couple the incident solar photons into the thin-film absorber layer are mandatory for high efficiency solar cells via anti-reflection and light trapping. In the past, a multilayer antireflection coating (ARC) was commonly used to reduce the surface reflection. However, issues related to material selection, thermal mismatch and instability of the thin-film stacks remain major obstacles to the application of such broadband and angle-independent antireflection coatings in solar cells [6]. Light trapping is another way to increase the absorption, utilizing geometries to increase the optical path of the photons near the band edge of the photo-active layer. Several works were done by utilizing structures to provide light trapping in thin film cells [7–11]. Some of previous works on light trapping focused on engineering the backside structures, which scatter or diffract the incompletely absorbed photons to oblique angles and hence increase the propagation length within the absorption layers [12–15]. In previous studies, engineering the backside structure enables only the light trapping mechanism, which primarily enhances the absorption of long-wavelength photons. However, the frontal structure not only provides forward scattering for light trapping, but also facilitates light transmission, which in turn improves the absorption in both, the short and long wavelength ranges. Previously reported textured metal back-electrodes also suffer from substantial loss owing to surface plasmonic absorption, which cancels

Abbreviations: ARC, antireflection coating; AOIs, angles of incidence; QPS, quasi-periodic structure; PS, polystyrene.

* Corresponding author. Tel.: +886 3 5712121x56357.
E-mail address: yup@faculty.nctu.edu.tw (P. Yu).

1566-1199/$ - see front matter © 2011 Elsevier B.V. All rights reserved.
doi:10.1016/j.orgel.2011.03.002

the absorption enhancement due to scattering [16–20]. Moreover, the backside structures do not increase the optical transmission at oblique angles of incidence (AOIs).

Herein, we present a quasi-periodic structure (QPS) on the indium tin oxide (ITO) anode, fabricated by scalable colloidal lithography. The ITO-QPS effectively couples the incident light to the photo-active layer via antireflection and light trapping mechanisms to boost the conversion efficiency of organic solar cells. Moreover, angle-resolved absorption spectroscopy reveals outstanding light coupling via ITO-QPS at large AOIs, promising omnidirectional and broadband light harvesting.

2. Experimental

The schematic illustration of the fabrication process is shown in Fig. 1. The ITO-QPS was fabricated with scalable colloidal lithography utilizing polystyrene (PS) nanospheres with a diameter of 600 nm as sacrificial masks. First, the PS spheres were spun-coated onto 260 nm thick ITO glass which self-assembled into a monolayer of closely-packed beads. A metal etcher (ILD-4100) was then employed to fabricate the ITO nanorod structure with BCl_3 = 100 sccm injection, pressure of 5 mtorr and an etching time of 170 s, which resulted in an ITO nanorod with a height of 100 nm. Removal of leftover PS was performed by dipping the ITO glass into acetone with sonification for 5 min. The scanning electron images (SEM) of the ITO-QPS before depositing the active layers are shown in Fig. 2a and b.

The glass substrate with ITO-QPS was then cleaned by ultrasonic treatment in detergents, including methanol, acetone and isopropyl alcohol, and finally dried overnight in an oven. Then, 12 nm PEDOT:PSS (Baytron P VP A1 4083) was spun-cast on the ultraviolet ozone-treated ITO. After annealing the PEDOT:PSS film at 120 °C for 30 min in the air, the sample was transferred to a glove box. The active material consisted of 2 wt.% RR-P3HT (Mw 3.7×10^4 g mol^{-1}) and 2 wt.% PCBM in a dichlorobenzene solution, obtained from Rieke Metals and Nano-C Inc., respectively.

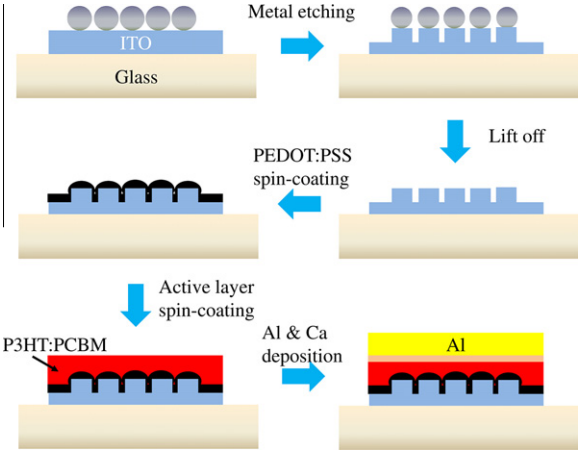

Fig. 1. The fabrication process of an organic solar cell with a patterned frontal electrode using colloidal lithography.

The solution blend was then spun-cast onto the PEDOT:PSS layer at a speed of 600 rpm for 60 s and then dried in covered Petri glass dishes for 30 min at room temperature. The thickness of P3HT:PCBM is 170 nm. Next, the semi-finished samples were baked on a hotplate for 30 min at 120 °C. Finally, 30 nm thick calcium followed by 60 nm thick aluminum was thermally coated onto the active material at a pressure of 6×10^{-6} torr through a 0.1 cm^2 shadow mask. The samples are prepared with a size of 20 × 50 mm and the results shown here are the averages of three samples.

Efficiency measurements were performed under simulated AM1.5G irradiation (100 mW/cm^2) using a Xenon lamp-based Thermal Oriel 1000 W solar simulator. The spectrum of the solar simulator was calibrated by a PV-measurement (PVM-154) mono-Si solar cell (NREL calibrated), and a Si photo diode with KG-5 color filter (Hamamatsu, Inc.) was used to check the irradiation of the exposed area (100 mW/cm^2). The PVM-154 combined with a KG-5 filter (350–700 nm passed, Newport) was used to simulate a reference solar cell with a spectral response from 350 to 700 nm, where the calibration was based on the IEC-69094-1 spectrum. *I–V* curves were measured with a semiconductor source measure unit (Keithley 2400) using a four wire connection and the measurements were corrected for the external series resistance. Stability in time is continuously monitored by routinely repeating the measurements on c-Si solar cells. The temperature of the cells was actively controlled during the measurements at 25 ± 1 °C.

The external quantum efficiency (EQE) system is equipped with a 450 W Xenon lamp (Oriel Instrument, model 6266) light source, a water-based IR filter (Oriel Instrument, model 6123 NS) and a monochromator (Oriel Instrument, model 74,100). The beam spot on the sample is rectangular, measuring roughly 1 × 3 mm. A calibrated silicon photodetector (Newport 818-UV) was used to calibrate the EQE system before measurements. A lock-in amplifier (Standard Research System, SR830) and an optical chopper controller (SR540), set in the voltage mode, were also equipped to lock the output signal and the photocurrent was converted to the voltage using a 1 ohm resistor, which was parallel to the sample. The temperature of cells was again actively controlled during the measurements at 25 ± 1 °C.

3. Results and discussion

Fig. 3 depicts the measured absorption and external quantum efficiency (EQE) spectra of organic solar cells with the ITO-QPS and with a flat ITO layer at normal incidence. The absorption measurement was carried out using an integrating sphere system to collect the scattered reflected photons. The superior absorption in the entire spectrum for the ITO-QPS cell is shown, especially in the wavelength range between 520 and 670 nm. The enhanced absorption results from the light coupling by the ITO-QPS, which serves both functions as the antireflection and forward scattering for light trapping. Inspection of the absorption and EQE spectra confirms that the enhanced carrier generation is contributed from the superior photon absorption.

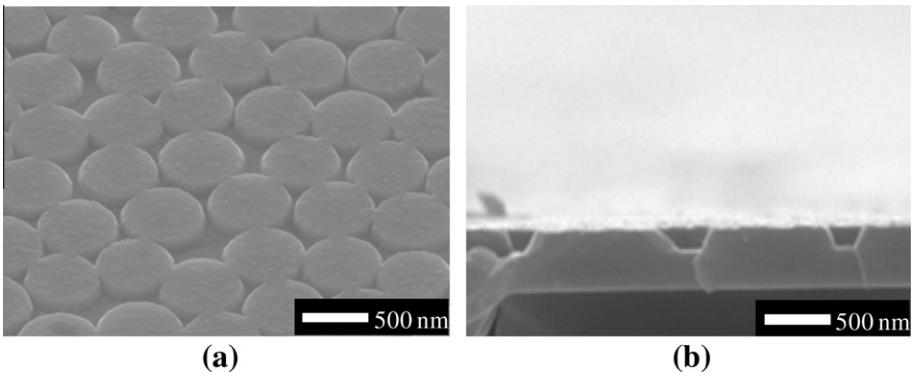

Fig. 2. The (a) top view and (b) cross-section SEM images of the ITO-QPS before the deposition of organic materials.

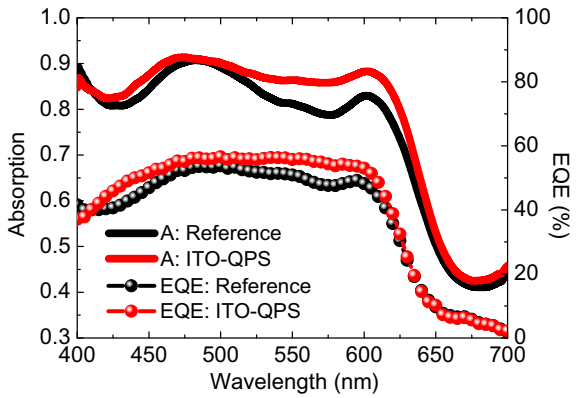

Fig. 3. Measured absorption and external quantum efficiency (EQE) spectra for the flat cell and the cell with an ITO-QPS.

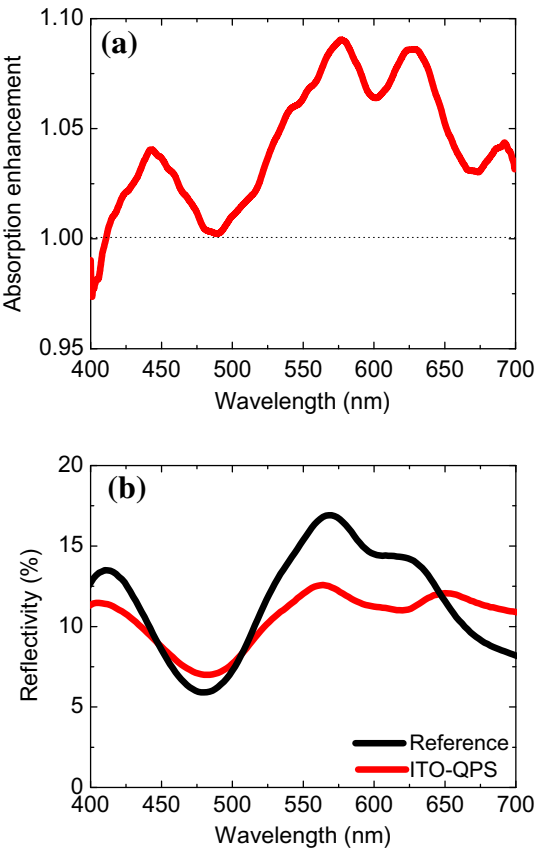

Fig. 4. (a) Absorption enhancement of the ITO-QPS cell to the reference. (b) Measured reflectivity of the devices without an Al back reflector.

The absorption enhancement by taking the ratio of absorption in Fig. 3 is plotted in Fig. 4a, which demonstrates a broadband improvement from 500 to 700 nm due to sufficient photon coupling by the frontal pattern. A required absorption length for different wavelengths can be calculated by $L = 1/\alpha$, where α is the measured absorption coefficient of P3HT:PCBM. The round-trip light propagation length is twice the thickness of P3HT:PCBM, approximately 340 nm, which corresponds to the absorption length for the 620 nm wavelength. The absorption enhancement in the spectrum region below $\lambda = 620$ nm, where the incident photons can be completely absorbed within a round-trip path length in the P3HT:PCBM layer, shows the antireflective property of the frontal ITO nanostructure. Forward scattering by the frontal ITO-QPS contributes to the absorption enhancement in P3HT:PCBM layer after $\lambda = 620$ nm. The measured reflectivity of the devices without Al back reflector is shown in Fig. 4b. In the wavelength range of $640 < \lambda < 700$ nm, the ITO-QPS device has higher reflection than the reference device before the Al back reflector deposition. However, after the deposition of Al back reflector, the absorption for the ITO-QPS cell was enhanced, which indicates the absorption enhancement (see in Fig. 4a) was contributed by light trapping. The enhanced absorption of the ITO-QPS cell reflects the boosting of the power conversion efficiency. The current density–voltage (J–V) characteristics for the reference and ITO-QPS cells under AM 1.5 conditions are shown in Fig. 5. The conversion efficiencies for the reference and ITO-QPS cells are measured at 2.91% and 3.26%, respectively. Compared to the reference cell, the ITO-QPS cell shows a 12% enhancement. This efficiency enhancement is contributed from the optical absorption, which results in an increase in the short-circuit current density,

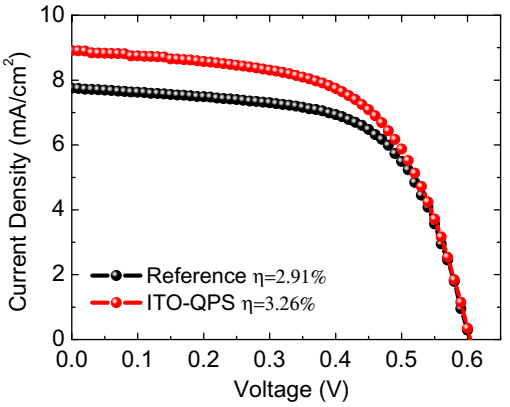

Fig. 5. Measured current–voltage curve of cells.

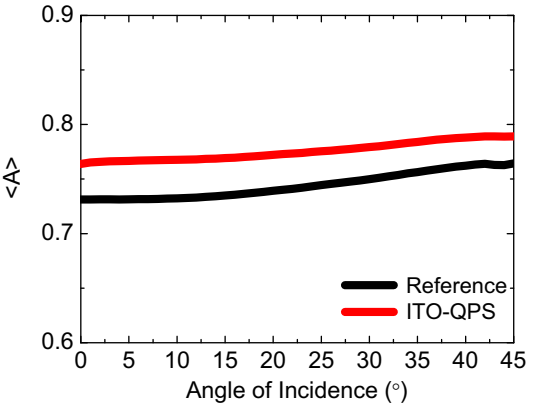

Fig. 7. Averaged absorption of the reference film and the ITO-QPS cell.

J_{sc} = 8.91 mA/cm^2 compared to the reference cell with J_{sc} = 7.75 mA/cm^2. The open circuit voltage V_{oc} of the ITO-QPS cell remains the same (0.6 V) and the deterioration of fill factors (from 63.6% to 61%) could result from the damaged ITO after metal etching.

The light harvesting at large angles of incidence is another key issue for thin film solar cells. The large-angle light harvesting of the cell benefits sufficient power generation in the daytime. Fig. 6a and b show the measured angle-resolved absorption spectroscopy of the reference cell and the ITO-QPS cell, respectively. Angle-resolved absorption spectroscopy is performed within the wavelength of 400 and 700 nm. However, only the wavelength range between 400 and 650 nm is shown, to reveal a clear contrast in the color maps. The measuring systems utilize a custom-built 15 cm radius integrating sphere with a motor-controlled rotational sample stage in the center and a randomly polarized broadband Xenon lamp to simulate the polarization state of sun light. The collection of reflected photons is then analyzed by a spectrometer (QE65000, Ocean Optics) to obtain the absorption spectrum with respect to different angles of incidence, of up to 45°. The system is calibrated by the reflective spectrum of a NIST-standard, intrinsic Si at normal incidence. Evidently, the angular absorption is enhanced by the ITO-QPS, especially in the range of $540 < \lambda < 620$ nm. The optical coupling at oblique AOI is tailed by the ITO-QPS, which modified the guiding conditions of the thin film layers. The coupling only takes place when the optical momentum of incident photons satisfies the guided modes of the ITO-QPS patterned films. We define a parameter, averaged absorption <A>, to express the capability of solar power harvesting by each cell:

$$< A >= \frac{\int_{400\,nm}^{700\,nm} A(\lambda,\theta) I_{AM1.5G}(\lambda) d\lambda}{\int_{400\,nm}^{700\,nm} I_{AM1.5G}(\lambda) d\lambda} \quad (1)$$

Where A(λ, θ) is the measured angular absorption spectrum, θ is the incident angle with respect to the normal surface, and $I_{AM1.5G}$ is the photon flux density of the solar spectrum [21]. We neglect taking the normal component of incident solar photon flux (i.e. $I_{AM1.5G}\cos\theta$) as varying the incident angle, to have a better understanding of the angular absorption of the patterned cells. Fig. 7 shows <A> with respect to the AOIs up to 45° for the reference cell and the ITO-QPS cell. The results illustrate that the ITO-QPS cell sufficiently absorbs the incident solar power at large AOIs. As seen in Fig. 7, the averaged absorption of the ITO-QPS cell does not rise as fast as the reference, indicating the insensitivity to the angles of incidence.

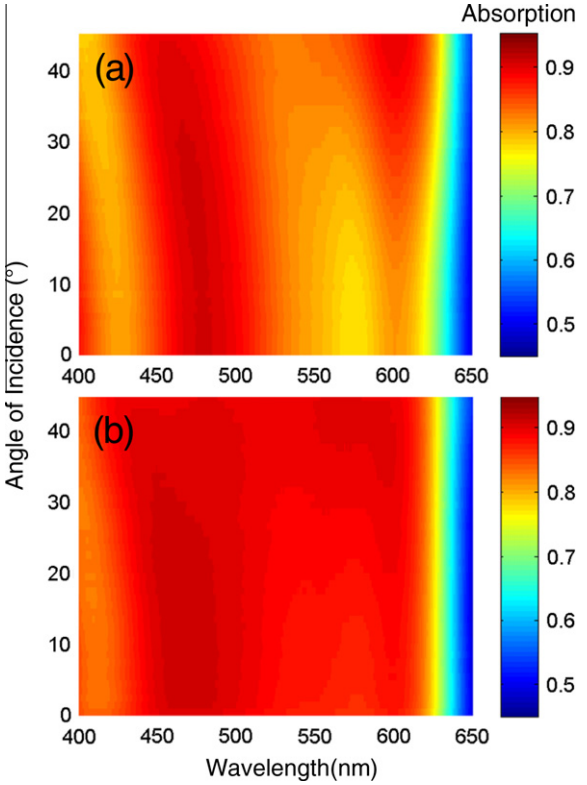

Fig. 6. Angular absorption spectra of (a) the reference cell, and (b) the ITO-QPS cell.

4. Conclusion

In conclusion, we have demonstrated thin-film organic solar cells with a frontal ITO quasi-periodic structure. The

ITO-QPS is fabricated by colloidal lithography, which is applicable for large scale production. The measured cell absorption spectra closely matches the external quantum efficiencies and results in power conversion efficiencies of 3.26% for the ITO-QPS cell, compared to a conversion efficiency of 2.91% for the reference cell. Angle-resolved absorption spectroscopy measurements also show enhanced light coupling at the cells at an oblique angle of incidence. This new design is not strictly relevant to organic based devices, but may be broadly applicable to other common thin-film solar cell materials systems such as a-Si:H, CdTe, and CIGS. This result can directly impact the attainment of the scalable green energy from thin-film solar cells.

Acknowledgment

The authors would like to thank Dr. Chung-Hsiang Lin for his technical support and helpful suggestions.

References

[1] J.M. Nunzi, C. R. Phys. 3 (2002) 523.
[2] L.A.A. Pettersson, L.S. Roman, O. Inganäs, J. Appl. Phys. 86 (1999) 487.
[3] T. Stübinger, W. Brütting, J. Appl. Phys. 90 (2001) 3632.
[4] A.P. Smith, R.R. Smith, B.E. Taylor, M.F. Durstock, Chem. Mater. 16 (2004) 4687.
[5] T. Aernouts, W. Geens, J. Poortmans, P. Heremans, S. Borghs, R. Mertens, Thin Solid Films 403 (2002) 297.
[6] P. Lalanne, G.M. Morris, Proc. SPIE 2776 (1996) 300.
[7] M. Niggemann, B. Zimmermann, J. Haschke, M. Glatthaar, A. Gombert, Thin Solid Films 511 (2006) 628–633.
[8] M. Niggemann, M. Riede, A. Gombert, K. Leo, Phys. Stat. Sol. A 205 (No. 12) (2008) 2862.
[9] S.B. Rim, S. Zhao, S.R. Scully, M.D. McGehee, Appl. Phys. Lett. 91 (2007) 243501-1–243501-3.
[10] K. Tvingstedt, S.D. Zilio, O. Inganas, M. Tormen, Optics Express 16 (No. 26) (2008) 21608.
[11] D.H. Ko, J.R. Tumbleston, L. Zhang, S. Williams, J.M. DeSimone, R. Lopez, E.T. Samulski, Nano Lett. 9 (No. 7) (2009).
[12] D. Zhou, R. Biswas, J. Appl. Phys. 103 (2008) 093102.
[13] L. Zeng, P. Bermel, Y. Yi, B.A. Alamariu, K.A. Broderick, J. Liu, C. Hong, X. Duan, J. Joannopoulos, L.C. Kimerling, Appl. Phys. Lett. 93 (2008) 221105.
[14] P. Bermel, C. Luo, L. Zeng, L.C. Kimerling, J.D. Joannopoulos, Opt. Express 15 (2007) 16986.
[15] N.N. Feng, J. Michel, L. Zeng, J. Liu, C.Y. Hong, L.C. Kimerling, X. Duan, IEEE T. Electron. Dev. 54 (2007) 1926.
[16] W. Wang, S. Wu, K. Reinhardt, Y. Lu, S. Chen, Nano Lett. 10 (2010) 2012.
[17] K. Tvingstedt, N. Persson, O. Inganäs, A. Rahachou, I.V. Zozoulenko, Appl. Phys. Lett. 91 (2007) 113514.
[18] R.H. Franken, R.L. Stolk, H. Li, C.H.M. van der Werf, J.K. Rath, R.E.I. Schropp, J. Appl. Phys. 102 (2007) 014503.
[19] F.J. Haug, T. Söderström, O. Cubero, V. Terrazzoni-Daudrix, C. Ballif, J. Appl. Phys. 104 (2008) 064509.
[20] J. Springer, A. Poruba, L. Müllerova, M. Vanecek, O. Kluth, B. Rech, J. Appl. Phys. 95 (2004) 1427.
[21] ASTMG173-03, Standard Tables for Reference Solar Spectral Irradiances, ASTM International, Conshohocken, Pennsylvania, 2005.